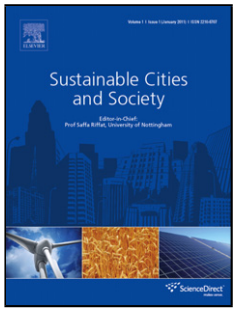
Accepted Manuscript



Title: Urban Morphology and Landscape Structure Effect on Land Surface Temperature: Evidence from Shiraz, a Semi-arid City

Authors: Abolghasem Azhdari, Ali Soltani, Mehdi Alidadi

PII: S2210-6707(18)30448-7
DOI: https://doi.org/10.1016/j.scs.2018.06.034
Reference: SCS 1168

To appear in:

Received date: 10-3-2018
Revised date: 19-6-2018
Accepted date: 25-6-2018

Please cite this article as: Azhdari A, Soltani A, Alidadi M, Urban Morphology and Landscape Structure Effect on Land Surface Temperature: Evidence from Shiraz, a Semi-arid City, *Sustainable Cities and Society* (2018), https://doi.org/10.1016/j.scs.2018.06.034

This is a PDF file of an unedited manuscript that has been accepted for publication. As a service to our customers we are providing this early version of the manuscript. The manuscript will undergo copyediting, typesetting, and review of the resulting proof before it is published in its final form. Please note that during the production process errors may be discovered which could affect the content, and all legal disclaimers that apply to the journal pertain.

ACCEPTED MANUSCRIPT

Urban morphology and landscape structure effect on land surface temperature: An evidence from a semi-arid city, Shiraz

Abolghasem Azhdari
MA in Urban and Regional Planning
Tarbiat Modares University, Tehran, Iran
Email: abolghasem.azhdari@modares.ac.ir

Ali Soltani*
*Corresponding author
Professor of Urban Planning & Transport
University of South Australia, Australia
K3-14, Kaurna Building, City West Campus
Tel: +61 8 8302 0333
Mob: +61 451439065
Email: ali.soltani@unisa.edu.au
http://people.unisa.edu.au/Ali.Soltani

Mehdi Alidadi
MA in Urban and Regional Planning
Tarbiat Modares University, Tehran, Iran
Email: m.alidadi@modares.ac.ir

Highlights

- Spectral, landscape and morphological variables had relatively strong correlation with LST.
- Bare lands, industrial and green spaces had a remarkable negative effect on LST.
- Residential areas with moderate and high building density alleviated the surface temperature.
- Dense gardens, lower road density, and more developed districts declined LST.

ACCEPTED MANUSCRIPT

Abstract

Urbanization process contributes to more urban climate changes specifically the land surface temperature (LST). Higher LST of urban areas compared to the surroundings is regarded as the side effect of urban morphology and landscape structure features. In this study, spectral and landscape indices and morphological variables (parcel density, housing density, road density, floor area ratio, mass-space proportion, land use pattern, and distance to CBD) are applied to investigate the correlation of urban morphology with LST. Landscape and morphological variables are provided from Landsat 5, statistical center of Iran and Shiraz's master plan and also gathered at the census district level. The results found that variables had relatively strong correlations with LST. While SHDI, DIVISION, FRAC, LSI, and road density had positive correlation coefficient, NDBI, housing and parcel density, FAR and mass-space proportion were negatively correlated. Moreover, examining land use pattern and its relation to LST revealed that bare lands, industrial and green spaces had a remarkable negative effect on LST. Also residential areas with moderate and high building density alleviated the surface temperature. Alongside that, dense gardens, lower road density, and more developed districts declined LST in Shiraz, a semi-arid urban environment in Iran.

Key words: Land Surface Temperature, Urban Morphology, Landscape Metrics, Landscape Structure, Land Cover and Land Use

1 Introduction

In the last decades, many cities have been facing massive socioeconomic changes and physical expansions (Ewing et al., 2002). The physical expansion of cities which is mainly identified as urban sprawl has had critical effects on urban morphology of metropolitan areas (Rahman et al., 2011). Although global warming is not the direct result of urbanization process and population growth (Grimmond, 2007) but, urban morphology is the main climate change driver (Petralli et al., 2014) in smaller scale (Edussuriya et al., 2011). Changes in transmittance and evaporation of land covers are the side effect of changing urban morphology which consequently alter thermal characteristics of the land surface (Hu & Jia, 2010; Dihkan et al., 2015). These thermal changes will lead to temperature differences between cities and their surrounding rural areas (Sheng et al., 2017). However, due weakness of mutual dialogue between climatology and planning (Oke, 1984) the results of climatology researches have been far from applicable planning practices (Alcoforado et al., 2009; Xu et al., 2017). Thus, urban climatology or urban meteorology have experienced a paradigm shift to analyze climatic effects of urbanization (Mills, 2014) by planning parameters (Petralli et al., 2014). New urban climatology is basically set on built environment (Hebbert, 2014) and the way citizens use it (Privitera et al., 2018).

One of the main climatic effects of urban development is to have higher temperature compare to the surrounding (Moonen et al., 2012), which is measured by either air or surface temperature (Luo et al., 2018) in urban spaces. Nevertheless, atmospheric temperature fails to describe the spatial variation of temperature differences between an urban area and the surroundings since there is usually a single temperature value for the whole study area. However, calculating land surface temperature through remote sensing imagery gives us the opportunity to capture the surface temperature of different parts of an urban area (Sheng et al., 2017).

In addition, the temperature difference between an urban area and the surroundings in temperate and sub-tropical climates is different from more arid environments. While in former it is generally positive, in latter there is a possibility for urban areas to have a lower temperature than the surroundings; a phenomenon that is called surface urban cool islands (SUCI) or surface urban heat sink (Frey et al., 2005; Lazzarini et al., 2013). It means urban expansion can generally decrease land surface temperature in more arid urban environments.

It is confirmed that thermal changes influence planning issues such as water and air quality (Kahya et al., 2016), health affairs (Grimmond, 2007; Dugord et al., 2014), and energy consumption (Salat, 2009; Clinton & Gong, 2013; Morganti et al., 2017). On the other hand, urbanization process and landscape conversion potentially affect ecologic and climatic variables (Weng et al., 2007; Salat, 2009; Hu & Jia, 2010; Zhou et al., 2011; Dihkan et al., 2015; Sheng et al., 2017) particularly the atmospheric and surface temperature of urban areas (Bokaie et al., 2016; Tsirigoti & Bikas, 2017; Privitera et al., 2018). In other words, urban morphology which is a part of planning sphere, has a high correlation with air and surface temperature variation (Weng

ACCEPTED MANUSCRIPT

et al., 2007; Boukhabla et al., 2013; Wu et al., 2014; Petralli et al., 2014; Guo et al., 2016; Xu et al., 2017; Tong et al., 2018).

Despite the long history of urban morphology in different disciplines, (Lilley, 2009) and its four main schools in urban planning (Whitehand & Gu, 2010), it is not clearly explained in the context of urban climatology. The characteristics of urban morphology are elucidated by various aspects of the landscape such as geometry, natural and built-up areas and densities, urban fabric configuration (Yu et al., 2009; Zhou et al., 2011) and composition (Buyantuyev & Wu, 2010; Weng et al., 2007), street patterns, and land uses (Thani et al., 2013; Petralli et al., 2014). Due to vantage of data availability of urban morphology variables (Xu et al., 2017), it can be applied in four scales: the region, the city, the district and the building which reflect human activity in space (Yu et al., 2009; Edussuriya et al., 2011). Although the relationship between temperature and landscape characteristics of the cities are over studied (Robinson, 2006; Zhou et al., 2011; Wei et al., 2016; Zhou et al., 2017), some problems remained unsolved by both numerical (Allegrini et al., 2015) and statistical modeling (Edussuriya et al., 2011). Firstly, while they have investigated the relation between LST and urban morphology Wei et al. (2016), they mainly focused their attention on urban design and building characteristics in neighborhood scale (Robinson, 2006; Barau et al., 2015; Xu et al., 2017; Zhou et al., 2017), secondly, they have declined the concept of urban morphology into physical form (Yu et al., 2009; Zhou et al., 2017; Tsirigoti & Bikas, 2017; Tong et al., 2018), and last, the difference between land use and land cover is not fully determined (Hu & Jia, 2010), except for few studies (Emmanuel & Johansson, 2006; Edussuriya et al., 2011),; the former is functional and can't be measured by remote sensing techniques.

Urban morphology has two main sections, physical and functional; the former can be covered by studying urban landscape structure and physical arrangement, but the latter should be drawn in spatial variables context. The present study aims to examine the physical aspect of urban morphology at the census district level. Methodologically, urban landscape structure can be traced by landscape metrics (Weng et al., 2007; Wu et al., 2014) and physical arrangement of urban morphology can be explained by land use, and other human-related variables such as parcel density, housing density, and so on.

Shiraz is built over a green plain of the Zagros Mountains and is known as the city of gardens. Environmental characteristics of the city and its historic gardens have influenced urban climate (Soltani & Sharifi, 2012) and housing pattern (Ardeshiri et al. 2016). But the drought of the last decade, along with the widespread expansion of the city towards natural and rural areas (Bagheri & Tousi, 2018), as well as the loss of a significant part of vegetation over the past few decades (Sarvestani et al., 2011), have made Shiraz a drier city than ever before. Thus, Shiraz as a semi-arid urban area is chosen to analyze land surface temperature and its relation to urban morphology parameters at the census district level. Land surface temperature (LST) was measured by RS technics in Shiraz in order to retrieve mean LST for each district of the city and then study its relationship with urban morphology of various districts. In addition, urban morphology is translated into two main categories, landscape variables (spatial composition and configuration) and physical variables which include land use, density functions, and other human-related form characteristics. Therefore, the main question raised by this study is how the district-level urban morphology of a semi-arid urban environment should be arranged in order to minimize land surface temperature.

2 Methodology

2.1 Case study

Shiraz, the fifth largest city of Iran in terms of population and a notable economic, social, political and administrative center, is located in the south Iran (Fig. 1). The latest administrative area of the city occupied 43725 hectares, and the metropolitan area population, which included the city and surrounding rural areas, as well as Sadra new town, was 1.869 million (2016 census). The annual population and area growth rate of the city over the past three decades have been 2.04% and 3.16% respectively. Shiraz's climate is generally classed as a hot semi-arid climate according to the K¨oppen climate classification (Peel et al., 2007) and has a hot summer with a July average high of 38.8 °C. However, due to some environmental features, such as Zagros Mountains overlooking the city, together with Maharloo Lake at the east side of Shiraz, winter is usually cold in this urban area. The height of Shiraz ranges from 1,488 meters above sea level in the far eastern part, to 1,700 meters in the far northwestern part of the metropolitan area.

ACCEPTED MANUSCRIPT

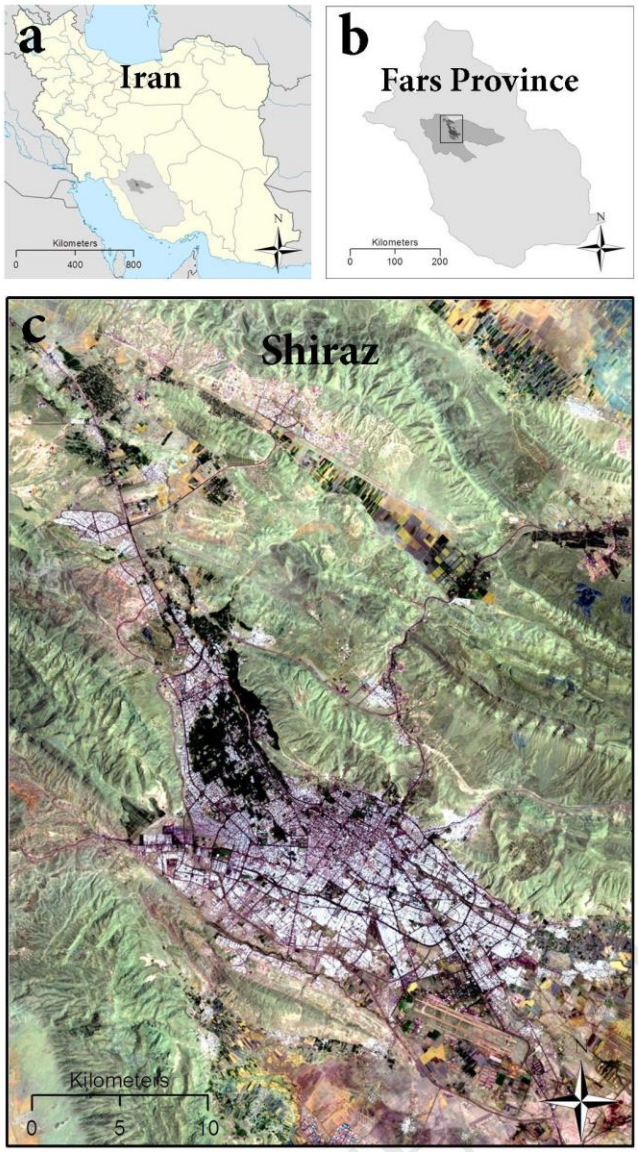


Figure 1: a, Fars province location in Iran; b, Shiraz county location in Fars province; c, Shiraz City

2.2 Data acquisition

In order to retrieve the land surface temperature and to classify different land covers, four satellite images acquired by Landsat 5 Tm on 28 March, 18 July, 22 October, and 7 January 2011 were obtained from United States Geological Survey (USGS). After the geometric and radiometric correction of images, the image classification process was conducted by using Maximum Likelihood method which has shown to have better performance than other algorithms (Ali et al., 2017).

Different types of land covers were classified into three general classes of soil, vegetation and impervious surfaces. The kappa coefficients were also used to verify the accuracy of the classified images and they ranged between 84.1% and 89.6%. An accuracy greater than 80% is usually considered adequate by studies for further analysis (Zhou et al., 2014; Bokaie et al., 2016). Data needed to study urban morphology of Shiraz, including building density and land use categories, were obtained from the 7th Iranian National Census in 2011 and Shiraz Comprehensive Plan. The census data in Iran is presented at district and block level. As urban morphology can be studied at different levels, we chose the district level data to study the relationship between LST and urban morphology. Shiraz has more than 500 districts, and independent variables demonstrate the urban morphology of each district. Also a single mean value of LST was assigned to each district for each season and then in order to conduct Pearson's correlation and regression analysis, the

ACCEPTED MANUSCRIPT

average value of the mean LSTs calculated for four seasons was used. Afterwards, we investigated the effect of each variable on the mean LST of districts.

2.3 Retrieval of LST

The thermal bands of the images (band 6 of Landsat TM) were used to derive LST for each year. First, to estimate the LST, the Digital Numbers were converted to radiation values to obtain the Top of Atmospheric (TOA) as below (Chander & Markham, 2003):

$$L_\lambda = \frac{L_{Max,\lambda} - L_{Min,\lambda}}{Q_{Cal,Max} - Q_{Cal,Min}} . (Q_{Cal} - Q_{Cal,Min}) + L_{Min,\lambda} \quad (1)$$

where the Lλ is the spectral radiance at the sensor's aperture in W/(m2.sr.µm), Qcal is the quantized calibrated pixel value in DNs, Qcalmin is the minimum quantized calibrated pixel value, and Qcalmax is the maximum quantized calibrated pixel value; LMINλ is the spectral radiance scales to Qcalmin, LMAXλ is the spectral radiance scales to Qcalmax.

Next, the surface-leaving radiance was acquired from TOA radiance (Sobrino et al., 2004):

$$L_{TOA} = \tau\varepsilon L_\tau + L_U + (1 - \varepsilon)L_d \quad (2)$$

Where LTOA is the at-sensor radiance or Top of Atmospheric (TOA) radiance, τ is the total atmospheric transmissivity between the surface and the sensor, ε is the land surface emissivity, Lτ is the radiance of a blackbody target of kinetic temperature T, LU is the upwelling atmospheric radiance, and Ld is the downwelling atmospheric radiance. The atmospheric transmission, and the upwelling, and downwelling radiance values were obtained using the Atmospheric Correction Parameter Calculator online tool which takes altitude, pressure, air temperature and humidity into account to calculate τ, LU and Ld (Barsi et al., 2003).

The land surface emissivity (LSE) which is one of the essential parameters to retrieve LST (Li et al., 2016) were calculated for the thermal band with the simplified of Normalized Difference Vegetation Index (NDVI) Thresholds Method ($NDVI^{THM}$). According to this method, certain NDVI thresholds are used to identify soil pixels ($NDVI < NDVI_S$), full vegetation pixels ($NDVI > NDVI_V$), and mixed pixels ($NDVI_S \leq NDVI \leq NDVI_V$) from one another ($NDVI_V = 0.5$ and $NDVI_S = 0.2$) (Keramitsoglou et al., 2011). To sum up, the land surface emissivity was calculating according to the below formulas proposed by (Sobrino et al., 2004):

$$\varepsilon = \varepsilon_V P_V + \varepsilon_S(1 - P_V) + d_\varepsilon \quad (3)$$

where ε_V is the vegetation emissivity (0.99) and ε_S is the soil emissivity (0.96), P_V is the vegetation proportion as below:

$$P_v = \left[\frac{NDVI - NDVI_{min}}{NDVI_{max} - NDVI_{min}}\right]^2 \quad (4)$$

Where $NDVI_{max} = 0.5$ and $NDVI_{min} = 0.2$.

At the end, surface-leaving radiance was converted to surface temperature by assuming the earth's surface is a black body (Tran et al., 2017):

$$T = \frac{K_2}{\ln(\frac{K_1}{L_T} + 1)} \quad (5)$$

where T is the brightness temperature in Kelvin, K1 and K2 are the calibration constants and L − T is the radiance of a blackbody target of kinetic temperature T. The final land surface temperature map was converted from Kelvin to Celsius degrees.

ACCEPTED MANUSCRIPT

2.4 Urban morphology, landscape structure

2.4.1 Landscape composition

Spectral indices are efficient indicators to investigate the relationship between LST and land covers as they explore reflectance values as of various land cover types (Ali et al., 2017). NDVI, as one of the most widely-used indices in environmental studies (Bokaie et al., 2016), can efficiently represent the effect of vegetation fraction on LST (Ogashawara & Bastos, 2012). Investigating the effect of non-vegetative land covers which is impervious surfaces in this study, on LST has also attracted a great deal of attention in previous studies (Chen et al., 2006; Kikon et al., 2016). NDBI which is sensitive to the built-up area is efficient to analyze the pattern of the impervious surfaces (Zha et al., 2003). These two spectral indices which are measuring the abundance of vegetation and non-vegetative land covers in each district along with three landscape metrics were chosen in order to study the relationship between landscape composition and the mean LST of districts.

There are a great number of landscape metrics to investigate the configuration and composition of land covers. However, many of them overlap due to the same input data. Thus, four landscape metrics (McGarical et al., 2012) were chosen based on the theoretically and practically importance of them (Li & Wu, 2004) to analyze the linear regression between LST and the abundance of impervious surfaces, diversity and shape complexity of land covers in each district. NDVI and NDBI show us how increase or decrease in land covers areas affected the mean LST in each districts and SHDI examines the effect of the proportion of landscape occupied by built-up areas compared to other land covers (Tab. 1).

2.4.2 Spatial configuration

Previous studies have reported that shape complexity and fragmentation of land covers have a notable influence on LST (Li et al., 2011; Connors et al., 2013). There are several indices to calculate the spatial configuration (Yu et al., 2009; Zhou et al., 2011) but here three well-established metrics were used. Landscape Shape Index (LSI) and Fractal Dimension Index (FRAC) measure the shape complexity of land covers by studying the relative amount of perimeter per unit area, and Landscape Division Index (DIVISION) (McGarical et al., 2012) is the third spatial configuration index to study the degree to which land covers are broken up into separate patches and how an increase in the value of the built-up fragmentation in each district can affect LST (Tab. 1).

2.5 Urban morphology, physical arrangement

Urban morphology characteristics in previous studies have interpreted in different ways (Mills, 2014). As discussed in section 1, depend on the background of the researcher (Yu et al., 2009), the scale of study (Robinson, 2006; Edussuriya et al., 2011; Allegrini et al., 2015), data availability (Xu et al., 2017), and topical (Privitera et al., 2018) and thematic (Boukhabla et al., 2013; Guo et al., 2016) focus of the research factors have changed. The distinction between landscape and morphology (Barau et al., 2015) is clarified in this study. So, morphological variables are those characteristics in which are related to human functions such as architecture, urban design and infrastructure, human activities, socio-demographic features (Salat, 2009), etc. To cover these dimensions of the morphological structure of Shiraz metropolitan, as shown in tab. 1, density variables (road density, housing and parcel density), building (FAR) and block level features (mass-space proportion), the total structure of the city (distance to CBD), and land use pattern are applied. RD, HD, PD, and FAR functions are presented in tab. 1, Euclidean distance to CBD reflects the importance of proximity to city center, and land use pattern provides information about the distribution of activities through the city.

2.6 Methods

In order to analyze the relationship between LST and urban morphology, Pearson's correlation, linear and exploratory regression are applied. The former reflects the bilateral relation of variables, and the latter investigates the causal relation (Alidadi & Dadashpoor, 2018) of morphological variables to LST. Pearson's correlation is calculated in Spss 22. Linear regression is estimated by ordinary least square (OLS) in Excel 2013, and exploratory regression is based on ArcMap 10.2 spatial analyst extension. The 3-d figures are mapped in ArcScene 10.2. Regression analysis is applied for all variables except land use pattern. Eleven different land uses (Tab. 1) are the independent or explanatory variables and LST is the dependent variable.

ACCEPTED MANUSCRIPT

The objective is to determine which single land use or combination of land use categories can better explain the LST pattern.

Table 1. Spectral and landscape indices selected in this study

Type	Index (abbreviation)	Description (unit) and range	Equation	Input data
Landscape Composition	Normalized Difference Vegetation Index (NDVI)	A measure of the abundance of vegetation in the landscape. (none) -1 ≤ NDVI ≤ 1, with higher values indicating more vegetation	$\frac{(\rho_{NIR} - \rho_R)}{(\rho_{NIR} + \rho_R)}$	Band 3 and 4 of Landsat TM sensor
	Normalized Difference Built-up Index (NDBI)	A measure of the abundance of built-up area in the landscape. (none) -1 ≤ NDBI ≤ 1, with higher values indicating more built-up area	$\frac{(\rho_{SWIR\ 1} - \rho_{NIR})}{(\rho_{SWIR\ 1} + \rho_{NIR})}$	Band 4 and 5 of Landsat TM sensor
	Shannon's Diversity Index (SHDI)	A measure of the diversity of land covers (none) 0 ≤ SHDI < 1	$-\sum_{i=1}^{m} P_i ln P_i$	Vegetation cover Soil cover Impervious surface
Spatial configuration	Landscape Shape Index (LSI)	The total length of edge divided by the shortest possible edge length for the area of a patch. It increases as the shape of a patch becomes more irregular. (None) LSI ≥ 1, without limit	$\frac{0.25.\sum_{k=1}^{m} e_{ik}^*}{\sqrt{A_i}}$	Vegetation cover Soil cover Impervious surface
	Fractal Dimension Index (FRAC)	A measure of departure from Euclidean geometry. As the patches become more complex, FRAC increases. (none) 1 ≤ FRAC ≤ 2	$\frac{2\ln(0.25p_{ij})}{lna_{ij}}$	Impervious surface
	Landscape Division Index (DIVISION)	A measure of the fragmentation of land covers. DIVISION deals with the degree to which the landscape is broken up into separate patches. (proportion) 0 ≤ DIVISION < 1	$\left[1 - \sum_{j=1}^{n} \left(\frac{a_{ij}}{A_i}\right)^2\right]$	Impervious surface
Morphological indices	Road Density (RD)	An indicator for measuring the density of roads. The bigger this indicator, the wider of the roads.	$\frac{R_i}{A_i}$	Vector data
	Housing density (HD)	An indicator for measuring the proportion of residential area in the district. A higher value for this indicator means that districts are more residential.	$\frac{H_i}{A_i}$	Vector data
	Parcel Density (PD)	The number of parcels per hectare. It is an index measuring the size of parcels in statistical areas. (Number per hectares) PD > 0	$\frac{n_i}{A_i}(10000)$	Vector data
	Floor area ratio (FAR)	An indicator for building density measurement. The higher the indicator, the greater the use of land will be.	$\frac{\sum_{j=1}^{m} M_j}{H_i}$	Vector data
	Mass-Space Proportion (MS_P)	An indicator for measuring the ratio of open space to usable areas. The higher the indicator, the lower the amount of open space in the district.	$\frac{M_i}{S_i}$	Vector data
	Distance to CBD (Dist_CBD)	Distance between the center of districts and CBD.	_____	Vector data
	Land-use Pattern (LU_P)	A total of 8 different land uses were chosen to examine the effect of land use pattern on LST. These include: Mixed-use, agricultural, industrial, public facility, park, protected area, bare land, and residential (with 4 different building density)	_____	Vector data

ρ_R, band 3 (Red); ρ_{NIR}, band 4 (Near Infrared); $\rho_{SWIR\ 1}$ is band 5 (Shortwave Infrared); a_i, area of patch i; A_i, area of district i; p_i, proportion of the district i occupied by land cover i; eik*, is total length (m) of edge in district i between land covers i and k; R_i, area of roads in district i; H_i, residential area of district i; n_i, number of separate parcels in district i; M_i, usable area of the ground floors in district i; M_j, usable area of all floors in district i; S_i, area of open spaces in district i.

3 Results

3.1 LST of Shiraz and the variation of SUCI intensity

As mentioned, one of the characteristics of cities in arid or semi-arid environments is that the surface temperature of the built-up area is higher than of the surrounding. In order to indicate the temperature

ACCEPTED MANUSCRIPT

difference between urban and surrounding rural areas, the surface urban cool island intensity (SUCII) is usually measured (Zhang & Wang, 2008), but there is no definite method to do so (Rasul et al., 2015). A 5 or 10-km rural buffer around the core urban area which does not include other urban areas or water bodies is usually selected to compute the urban heat differential. In this study a 10-km buffer was selected to identify the surface urban cool island phenomenon in Shiraz for four different seasons. The difference in the temperature of the city and its surroundings in 2011 shows that the city's surface temperature was lower throughout the year (Tab. 2 and fig. 2). However, as seen in previous studies, this phenomenon reached its peak in summer in Shiraz as well. So what is clear is that built-up areas have had a positive effect on reducing the surface temperature of the city in general.

Table 2: LST description of Shiraz city and surrounding in four apt dates

Season	Spatial area	Minimum	Maximum	Mean	St.D	SULI intensity
Spring	Urban	8.03	41.67	23.00	3.72	3.49
	Surrounding	9.08	41.07	26.49	3.22	
Summer	Urban	26.57	56.42	40.77	4.40	6.23
	Surrounding	25.93	65.35	47.01	3.80	
Autumn	Urban	12.55	37.65	23.99	3.70	4.58
	Surrounding	9.96	43.93	28.58	3.97	
Winter	Urban	3.26	28.91	14.19	2.94	3.42
	Surrounding	0.41	29.43	17.61	3.78	

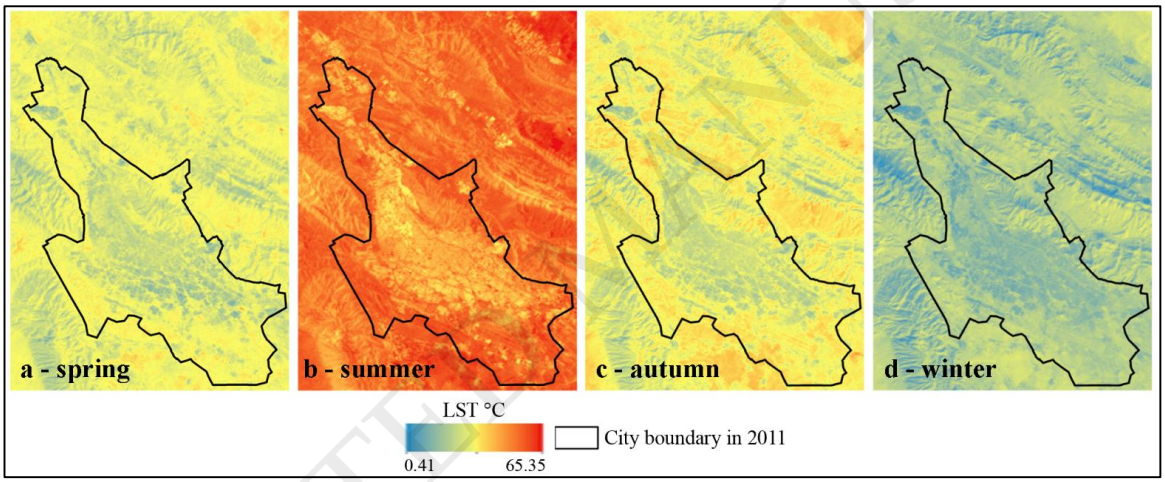


Figure 2. Temperature differences between Shiraz urban area in 2011 and the surroundings

3.2 Landscape structure of Shiraz and its effects on LST

3.2.1 The effect of land covers on LST

In this section, the relationship between the composition of land covers in each district and LST was studied. Surprisingly, the NDVI had a small positive relationship with the surface temperature in the study area (Tab. 3). However, most of the districts had the mean values of NDVI less than 0.05 and a great deal of vegetation of the study area is within conservation areas in a few districts (Figure 3a) so this result may not be so reliable. Therefore, in the following sections, we have further investigated the issue with a detailed examination of the impact of agricultural lands, urban parks and protected gardens on LST. As shown in fig. 3b, districts with the highest NDVI value have lower LST.

On the other hand, the NDBI represented a significant effect of the built-up area on reducing LSTs (Tab. 3). In other words, the higher the NDBI, the lower LST of the urban area (Fig. 3c).

To better understand the impact of urbanization on the formation of urban cool islands, landscape metrics were used. SHDI shows landscape diversity by examining the contribution of each land cover and it demonstrate a very strong positive correlation of 0.714 between LST and landscape diversity (Tab. 3). It can

ACCEPTED MANUSCRIPT

be seen that the greater the diversity of land covers in the district, the higher mean LST (Fig. 3d). These three indicators indicate that increasing the share of the built-up area in each district has had a significant effect on the reduction of the mean LST. In fact, as the landscape composition of district progressed towards urbanization, LST of districts reduced.

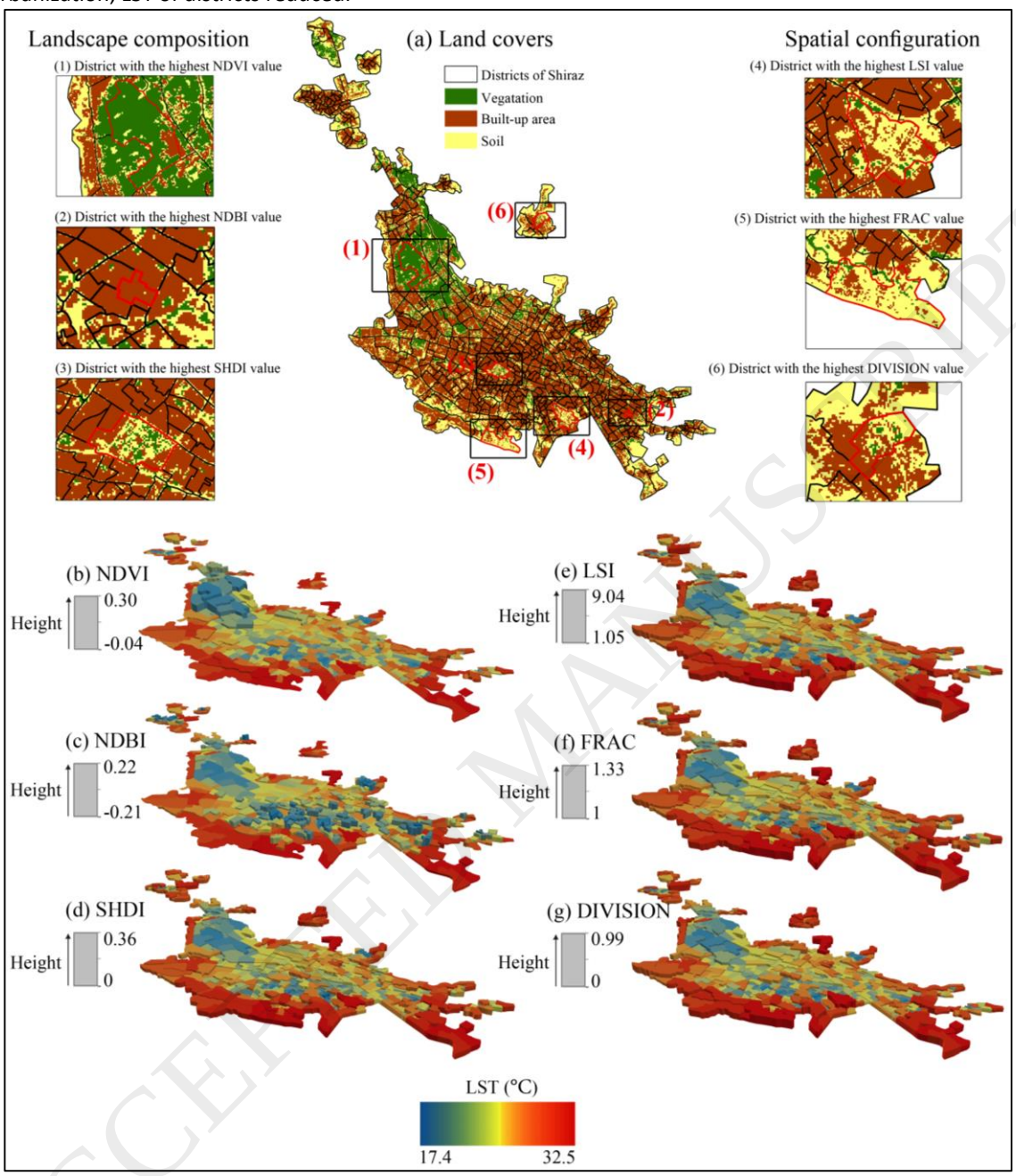


Figure 3. a, land cover pattern of Shiraz's districts based on 3 different land covers; b-g, 3-d figures of LST and landscape indices.

3.2.2 The effect of shape complexity and fragmentation of built-up areas on LST

The three landscapes metric considered to study the effect of the spatial configuration on LST generally examine the complexity of the urban patches and their fragmentation. LSI value clearly shows as the complexity of the urban patches or the proportion of the perimeter to the area of urban patches increased, the mean LST of districts rose as well (Fig. 3e). This indicator is sensitive to the size of the patches, meaning that as the patches are larger, the perimeter-area ratio varies. But FRAC can show the irregularity and complexity of urban patches, regardless of their size. FRAC indicates that LST increased as the urban patches

ACCEPTED MANUSCRIPT

of Shiraz indicated more departure from Euclidean geometry (Fig. 3f). This is due to the fact that as the perimeter-area ratio of a patch increases, the adjacencies with other land covers increase and the analysis of the composition showed that LST increased as the landscape became more diverse. And finally DIVISION examines the extent of dividing a land cover into several patches which indicates how fragmented a landscape is. This metric is good indicator to demonstrate how the mean LST increased as each district was made up of more fragmented urban patches (Fig. 3g). As shown in Tab. 3, except for NDVI, all the landscape indices had a strong correlation with the mean LST of districts.

Table 3: Pearson correlation of LST and landscape metrics in Shiraz (significant at 0.01 level)

	Metrics	Range	Std.Dev	Mean	Correlation with LST
Landscape composition	**NDVI**	-0.04<*D*<0.3	0.043	0.001	0.063
	NDBI	−0.2<*D*<0.22	0.075	0.030	-0.57
	SHDI	0.01<*D*<0.36	0.106	0.228	0.714
Spatial configuration	**LSI**	1.05<*D*<9.04	0.533	2.927	0.579
	FRAC	1.00<*D*<1.33	0.066	1.159	0.624
	DIVISION	−7.6<*D*<0.99	0.269	0.508	0.719

3.3 Physical arrangement of Shiraz's urban morphology and its effects on LST

Urban morphology as discussed in section 1 is interpreted variously in the literature. In this study, morphology refers to the spatial reflection of human activities such as road density, housing density, floor area ratio, parcel density, mass-space proportion, and distance to CBD (see fig. 2).

Road density, is a key indicator that shows the land volume allocated to streets, influences demand of urban travels (Soltani & Sharifi, 2012), higher CO2 emission, and asphalt cover of the land (Moonen et al., 2012). As shown in fig. 4a, road density in central parts of the city is considerably lower than the surroundings (due to mass transportation infrastructure construction by municipality farther from the CBD).

Housing density indicates the proportion of land used for housing purposes in a district, and explains the population distribution too. Fig. 4b illustrates the variation of housing density in Shiraz and how it is differently distributed in the center and periphery of the city. In the city center and Bazaar areas the index is high while in south and south-east it is remarkably low. Furthermore, northern parts of the city due to great volume of green spaces has lower housing density compare to the rest of the city.

Parcel density is the number of parcels built in a hectare of a district and illuminates the size of buildings in the city. A land can be occupied by a continuous building block or fragmented to small size ones and their climatic effect would be different. In Shiraz, as shown in fig. 4c, more parcels are located in a hectare of the central parts than of the outer rings of the city.

Floor are ratio shows the intensity of land used for buildings (one of the most common planning regulation and control tool); which takes both the height and volume of the building into account. This variable is calculated for all districts of the city and it ranges from 0.15 to 1.98 except for 3 zones and the average is around 0.98. As given in fig. 4d, there is no clear and recognizable pattern of FAR distribution through the city, but around the CBD the variable is lower than expected.

Mass-space proportion is an indicator that determines the ratio of open spaces to buildings in a district regardless of their land use and the construction height or volume. Previous studies have used the same indicators but in the present study it is remarkably accurate (the data is provided by municipality not by sampling). As shown in fig. 4e, the variable in the CBD has the highest value while the north and south of the city has the lowest value. This means that open spaces are mostly in the north and south of Shiraz and central parts of the city is mainly occupied by buildings and constructions.

And finally, distance to CBD is macro spatial variable that takes into consideration the importance of contiguity to the main congestion of employment in the city. In other words, according to traditional monocentric model of urban spatial structure, CBD is main congestion of employment and higher value of land price. Thus, higher population and building density, lower open spaces, greater parcel size, and higher M-S proportion are theoretically expected in this area.

Table 4: Pearson correlation of LST and morphological variables (significant at 0.01 level)

Variable	Range	Std.Dev	Mean	Correlation with LST
Road density	0.06<*D*<0.69	0.093	0.29	0.471
Housing density	0.02<*D*<0.82	0.178	0.44	-0.687

ACCEPTED MANUSCRIPT

Parcel density	0.03<*D*<116	18.68	24.54	-0.652
FAR	0.15<*D*<5.57	0.366	0.92	-0.497
M-S Proportion	0.04<*D*<5.26	0.818	1.63	-0.493
Dist. to CBD	0.1<*D*<21604	4692	7676	0.120

These 6 variables reflect the morphological feature of the Shiraz city. In this section the effect of these variables on LST is analyzed. To do so, the descriptive particularity of morphological indicators and the correspondent Pearson's correlation are calculated. From Tab. 4, some noticeable feature are needed to be mentioned. First of all, the range of variation of road density and housing density seems to be the same while parcel density has a standard deviation of 18.68. It shows that parcel density is a morphological factor that is highly varied through the city. Second, road density and distance to CBD, regardless of the correlation level, have a positive value while housing and parcel density, FAR, and M-S proportion are negative. Third, the highest values of R are for housing and parcel density by respect. Fourth, while there is variety of methodologies to assess the importance and effect of CBD on morphology of the city (Alidadi & Dadashpoor, 2018), the result of correlation demonstrate that CBD is not a critical variable to explain the urban climate in this study. Finally, variables with high negative correlation with LST are related to the morphology of urban districts. All of them are arrangement of morphological layout of buildings, land use and the combination of various planning issues. For example, housing density that has higher correlation with LST, compare to the rest, depends on planning variables such as land price, land use, socio-economic features, regulating and control criteria, and so on.

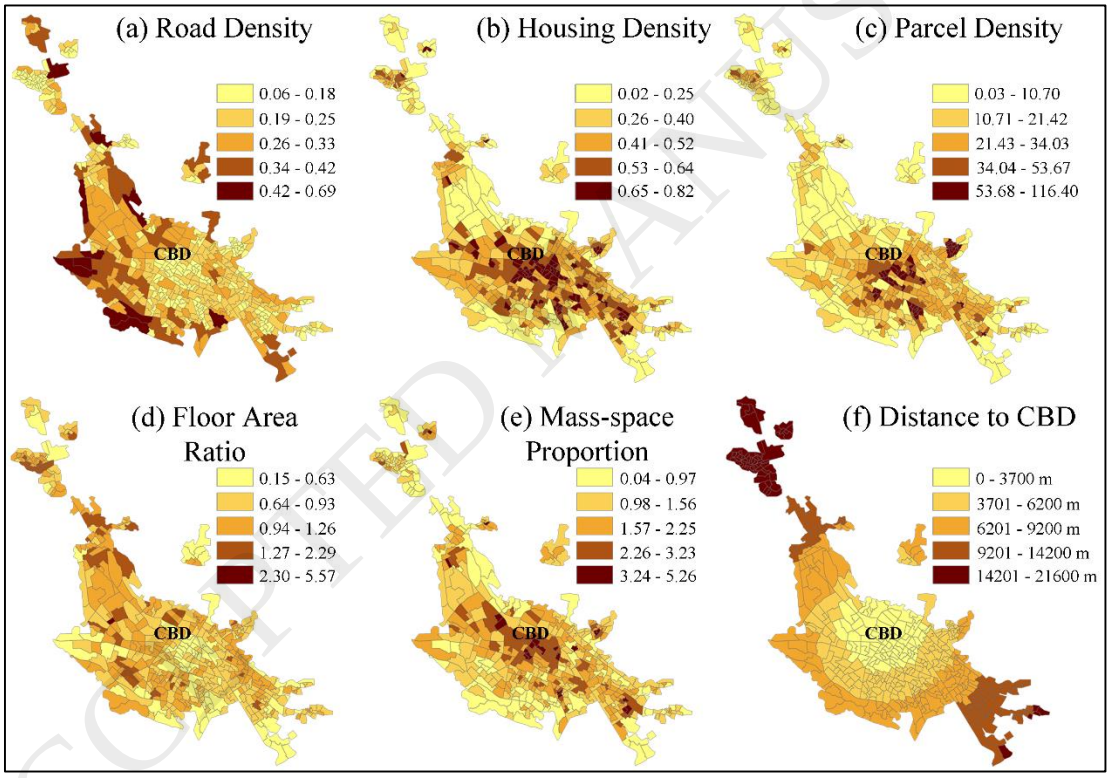


Figure 4: Variation of urban morphological indicators

3.3.1 Land use pattern and LST

The shape and abundance of land covers derived from the classification of satellite images showed the undeniable effect of the urbanization on a relatively large scale. However, it seems necessary to examine the role of urban land-use categories at a smaller level. In this study the contribution of seven different land use categories as well as four different residential areas with various building density (Fig. 5) to the intensification of LST was examined. The mean LST of agricultural land (47.2 °C) was higher than the temperature of other land use categories in Shiraz urban area. Industrial and bare land with a mean temperature of 45.3 °C were

ACCEPTED MANUSCRIPT

ranked second. Surprisingly, the mean LST of residential areas (38.3 °C) is less than public parks and protected areas with temperatures of 40.8 and 39.3 °C, respectively (Tab. 5). Perhaps this is why the correlation between the NDVI and LST was negligibly positive.

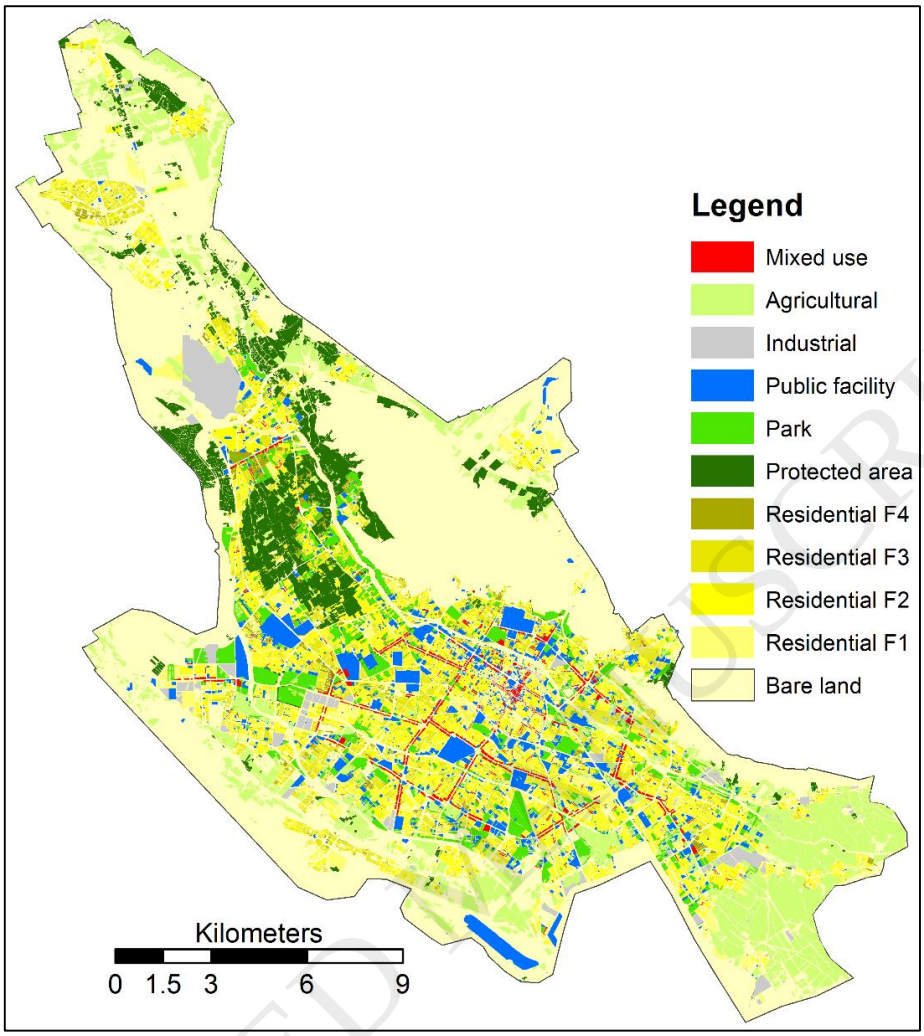


Figure 5. Land use types and floor area ration (FAR). Residential F1: FAR ≤ 0.7; Residential F2: 0.7 < FAR ≤ 1.25; Residential F3: 1.25 < FAR ≤ 1.7; Residential F4: 1.7 < FAR ≤ 5.6

But another remarkable matter to mention is that as the building density rose, LST decreased. Residential F4, which has the highest level of building density, has the lowest LST of 35.6 degrees while Residential F1 with the lowest building density has the highest LST of over 40 degrees (Tab. 5).

Table 5. LST of different land use categories in Shiraz urban area.

	Min (°C)	Max(°C)	Mean (°C)	STDEVA (°C)
Agricultural	29.77	56.00	47.26	4.01
Industrial	33.55	56.42	45.32	3.47
Mixed use	30.60	49.17	39.51	2.53
Public facility	26.57	54.32	42.69	4.20
Park	29.79	52.19	40.87	3.98
Protected area	28.19	53.90	39.21	5.87
Bare land	28.89	55.16	45.33	4.27
Residential F1	31.24	49.39	40.08	2.91
Residential F2	30.60	50.04	38.22	2.82
Residential F3	29.60	47.41	37.60	2.83
Residential F4	28.43	46.17	35.60	2.83

ACCEPTED MANUSCRIPT

However, the mean LST of land use categories does not indicate the importance of land uses in determining the mean LST of a district. In other words, it should be understood how much each land use contributes to the mean LST of a landscape or a district. By performing Exploratory Regression Tool in ARCGIS 10.2, different models were assessed with urban land use categories as independent variables and the average LST as the dependent variable and consequently passing models were obtained according to the criteria specified by the author (Tab. 6). A total of 16 different combinations of independent variables explaining the dependent variable passed all the criteria. Table 3 consists of three parts. Criteria, which shows the value obtained for each criterion for each passing model. Passing models, which contain properly specified OLS models, and, finally, a summary of variable significance that provides insight into the significance of variable relationships.

Table 6. Exploratory regression results with passing models and variable significance.

Number of Variables	Model Number	criteria						Passing Models
		AdjR2	AICc	JB	K(BP)	VIF	SA	
Two variables	Model 1	0.665	66.193	0.592	0.721	1.005	0.372	+Bare land*** -Residential F3**
	Model 2	0.652	66.755	0.644	0.850	1.003	0.366	+Bare land*** -Residential F2**
	Model 3	0.635	67.417	0.472	0.869	1.000	0.404	-Protected Area** +Bare land***
	Model 4	0.603	68.578	0.744	0.803	1.008	0.121	+Public facility* +Bare land***
Three variables	Model 5	0.831	60.363	0.660	0.368	1.002	0.855	+Industrial*** -Protected Area*** +Bare land***
	Model 6	0.828	60.583	0.736	0.461	1.012	0.965	+Industrial*** +Bare land*** -Residential F2***
	Model 7	0.826	60.740	0.721	0.657	1.023	0.983	+Industrial*** +Bare land*** -Residential F3***
	Model 8	0.807	62.180	0.274	0.860	1.050	0.950	+Park** +Bare land*** -Residential F2***
	Model 9	0.800	62.681	0.809	0.922	1.050	0.672	+Park** +Bare land*** -Residential F3***
	Model 10	0.798	62.843	0.778	0.874	1.051	0.985	+Park** -Protected Area*** +Bare land***
	Model 11	0.751	65.768	0.427	0.596	1.026	0.663	+Public facility* +Bare land*** -Residential F3**
	Model 12	0.743	66.187	0.444	0.429	1.021	0.730	+Public facility* +Bare land*** -Residential F2**
Four Variables	Model 13	0.863	62.428	0.773	0.787	1.050	0.931	+Park*** +Bare land*** -Residential F2*** -Residential F4*
	Model 14	0.862	62.479	0.578	0.529	1.140	0.502	+Industrial** +Public facility* +Bare land*** -Residential F2***
	Model 15	0.860	62.734	0.630	0.766	1.023	0.552	+Agricultural* +Industrial*** +Bare land*** -Residential F3***
Five variables	Model 16	0.896	65.504	0.948	0.793	1.051	0.417	+Agricultural* +Park*** +Bare land*** -Residential F2*** -Residential F4**

Summary of Variable Significance

	% Significant	% Negative	% Positive
Bare land	99.51	0.00	100.00
Park	39.39	8.50	91.50
Industrial	24.24	31.57	68.43
Residential F2	22.39	100.00	0.00
Residential F3	15.64	90.32	9.68
Protected area	11.34	35.00	65.00
Public facility	7.62	10.36	89.64
Residential F4	7.23	97.95	2.05
Agricultural	3.23	1.96	98.04
Mixed use	2.74	66.67	33.33
Residential F1	2.25	25.71	74.29

Table Abbreviations

AdjR2	Adjusted R-Squared > 0.5
AICc	Akaike's Information Criterion
JB	Jarque-Bera p-value > 0.1
K(BP)	Koenker (BP) Statistic p-value
VIF	Max Variance Inflation Factor < 7.5
SA	Global Moran's I p-value > 0.1

Model Variable sign (+/-)

Model Variable significance (* = 0.10, ** = 0.05, *** = 0.01)

No land use alone can fully explain LST. Although the summary of the variable significance indicates that bare land was 99.51 percent statistically significant and its relationship with LST was entirely positively stable. This means LST of districts almost always increased as the proportion of bare land grew up. All the 16 models had bare land as an exploratory variable. The next significant variable is public parks which was 39.3 percent statistically significant and had 91 percent positive stable relationship with LST. As mentioned, this is due to the presence of considerable open spaces in Shiraz's public parks.

Notable point is the 100 percent and 90.3 percent negative stable relationships of residential F2 and residential F3 with LST respectively. This means at all times residential F2 and F3 had a strong effect on mitigating LST. These two groups of residential areas were exploratory variables in 12 models. On the other hand, residential F1 with the lowest building density had 74.2 positive relationship with LST, but it did not contribute to any passing models. Therefore, future urban growth scenarios with low density is not an appropriate plan for Shiraz. Having a low variable significance (7.23), residential F4 was not a strong independent variable either in explaining LST and also confirmed the point raised in the previous section

ACCEPTED MANUSCRIPT

regarding the suitability of medium density development for Shiraz's residential areas in order to mitigate the urban heart island effect. Industrial was the third significant exploratory variable and had a positive relationship with LST at 68.4 percent of times. It was relatively an important variable for passing models. Protected areas containing Shiraz's public and private gardens had 65 percent positive relationship with LST and this might confirm the positive correlation between the NDVI and LST in the previous section. Although Agricultural land had a 98 percent positive relationship with LST, its significance in describing LST was negligible. Public facility and mixed use also had insignificant effect on LST.

At the end, the obvious matter is the undeniable role of bare land, industrial areas and public parks in increasing the mean LST of districts. And on the other hand, residential areas with medium and high building density as well as protected areas had the highest effect on mitigating LST in Shiraz urban area as a semi-arid urban environment.

4 Discussion

The issue of LST and its landscape and morphological causes are widely studied and their results have documented the meaningfulness of their relation. However, we should be aware that analyzing the relation is not a goal even a tool for planning purpose. Moreover, finding the operational variables that are under disposal of planners is necessary to be applicable in practical urban planning. Thus, in this study, important landscape and morphological indicators that are generally understandable to applicants chosen and tested in Shiraz.

4.1 The effect of landscape indicators on LST

Contrary to research on LST in both temperate and tropical climate urban environments (Ali et al., 2017; Bokaie et al., 2016; Ogashawara & Bastos, 2012), the NDVI had a small positive relationship with the surface temperature in the study area. However, the vegetation of Shiraz is mainly concentrated in the limited conservation area of the city called Ghasr-e-Dasht gardens. Therefore, by examining the relationship between land use pattern and LST, it was revealed that protected areas, as the main vegetation cover of Shiraz, had a significant effect on the reduction of LST, which is also obvious from 3-d figure of NDVI and LST (see fig. 3b).

The result also showed that impervious surfaces, which can be studied by NDBI, had a very strong relationship with LST. In fact, contrary to studies on LST of urban areas with temperate climate (Chen et al., 2006; Kikon et al., 2016) and in accordance with tropical climates (Ali et al., 2017), the horizontal expansion of the city will generally help to reduce LST of Shiraz. As shown in fig. 3c, districts with the highest NDBI value have the lowest LST. But the question is how this horizontal expansion should be to minimize LST. Should it be continuous or dispersed? Does urban open spaces have the same effect on LST as Buildings have? Does vertical expansion contribute to the reduction of LST?

Landscape metrics used in this study showed that as the urban landscape of districts became more integrated, LST decreased. Shannon diversity index revealed that growth in the diversity of land covers, which generally tend to increase the proportion of soil cover in a district, increased LST. Moreover, Division that calculates the degree to which a land cover is fragmented, indicated that dispersed expansion can increase LST compared to more continuous expansion. On the other hand, FRAC and LSI, which examined the shape complexity of build-up areas in this study, showed that if a land cover became more irregular and complex, the mean LST of a district would rise which is not the case in an urban area with temperate climate (Weng et al., 2007). More complexity means more adjacencies with soil cover and in section 3.3.1 we showed that soil cover had a very strong effect on the increase in LST. Therefore, in order to reduce the mean LST, urban landscape pattern of a district should be more continuous, integrated and dense, and less diverse, fragmented and complex and also open spaces of the district should be covered by as much vegetation as possible.

4.2 The effect of morphological variables on LST

In general, the temperature of the surface is affected by physical variables (Edussuriya et al., 2011; Morganti et al., 2017). Some of these variables have the applicability to be planned by developers or planners while others may be out of access or very hard to be controlled. In planning, specifically physical platform of the city, variety of socio-economics, geopolitics, regulative and other market forces are more or less influential.

ACCEPTED MANUSCRIPT

As shown in previous sections, morphological indicators that are planned directly by planners such as housing density, parcel density, FAR, and M-S proportion have a negative effect on LST while road density and distance to CBD are positively correlated with LST.

Housing density is the area of residential land use in a district and in city of Shiraz it is determined by master and detailed plan of the city. As given in Tab. 4, higher housing density had lower LST. However, this is just a linear correlation that means LST of districts with higher housing density is lower than of the rest of the regions.

Parcel density is calculated by dividing the number of parcels in a hectare. It is a planning regulator to separate an urban land into several parcels. As the number of parcels in a district increased, the surface temperature declined the same as Petralli et al., (2014) results in Florence. In Shiraz, historical zones of the city, that have smaller parcels the temperature is relatively lower than new big block zones. It is worth to mention that through these zones we witness the lowest rate of green spaces and road density. It is hard to conclude that smaller parcels definitely contribute to lower surface temperature, however, their correlation is strong and meaningful in a semi-arid climate zone. Also, Fig. 4c indicates that the farther from the CBD, the lower parcel density, while the temperature variation shows higher temperature in the outer rings, except for Ghasr-e-Dasht neighborhoods that is alleviated by mass green spaces.

M-S proportion that is a complementary variables calculates the share of mass to space in a district that is an indicator of open space ratio (Wei et al., 2016). The correlation between M-S proportion and LST indicates that as built-up to open spaces increased, the temperature declined (in central parts of the city the ratio of built-up area to open spaces is remarkably higher than the rest of the city).

One of the most common morphological variables that correlates with LST is floor area ratio (FAR). It is negatively correlated with LST (see Tab. 4); as FAR declined, the LST increased, to repeat again that is not a causal relation. FAR indicates the intensity of using a parcel through considering the number and area of the floors. FAR variation in the city shows higher value in the second ring and northern regions of the city that are planned and built in the last two decades. Guo et al., (2016) study in Guangzhou documented the same results by different variables, they used building density that is more or less the same as FAR and proved that as the density rises the LST declines. Distance to CBD is a macro-structure variable that explains the spatial structure of monocentric cities but does not have a strong direct correlation with LST.

5 Conclusion

While the association between physical form of the cities and their land surface temperature is undeniable, it is overstudied in the literature. However, this relationship is not straightforward and is highly dependent to atmospheric conditions, the texture of the city and other contextual variables. Moreover, most of these variables are somewhat complicated and cannot be understood by planners. Therefore, despite rich literature of the subject and improvement of calculations accuracy, professionals are skeptical to their applicability. Some simple understandable landscape and morphological variables, which can be controlled by planners in the planning action scale, are chosen and tested in Shiraz. Also it could be concluded that if we study the relationship between LST and urban morphology at the district level, which takes the whole city into account, then we might be able to derive some planning strategies to reduce LST effect.

Our results in this study indicated the correlation between urban landscape-morphology and LST in a semi-arid city, Shiraz. However, there are some surprising findings in detailed analysis of variables that support following remarks:

There is a clear distinction between landscape and morphological variables in nature, while the former is highly formal, the latter is about the use and arrangement of land through the city. Thus, these two arrays of variables are supplementary descriptive tools and statistical and mathematical simulation results should not be overestimated.

Macro-structure variables such as distance to CBD that is a popular spatial planning tool can't explain the dynamism of land surface temperature in urban scale while formal variables regarding the arrangement and variation of density and intensity of land uses are more applicable.

The housing density and the intensity of urbanized area were negatively correlated with the surface temperature, while open spaces increased the temperature. However, the effect of increasing the density on the reduction of LST will be conversed if the building density exceeds a certain level.

ACCEPTED MANUSCRIPT

Moreover, examining land cover patterns cannot fully explain the different uses of urban land and its relation to LST. Therefore, studying the pattern of land uses, which is usually provided by master plans, is necessary.

Horizontal expansion of cities in tropical environments should be as much continuous as possible and urban sprawl in its dispersed form should also be avoided. As to vegetation, urban open spaces should be supplemented by dense planting, especially in Shiraz which has vast urban parks.

To sum up, the development and expansion of cities is indispensable, however, with the principled planning, the expansion of cities can be directed to minimize the resulted undesirable environmental impacts. Therefore, in the present study we attempted to analyze the relationship between land surface temperature and Shiraz's urban morphology through its physical arrangement and urban landscape pattern. However, the formation of urban cool islands in a tropical environment through studying both atmospheric and surface temperature in a same study can further help planners to realize the best way to intensify urban cool island phenomenon in more arid urban environments.

References

1. Alcoforado, M.-J., Andrade, H., Lopes, A., & Vasconcelos, J. (2009). Application of climatic guidelines to urban planning: The example of Lisbon (Portugal). *Landscape and Urban Planning*, *90*(1), 56 – 65.
2. Ali, J. M., Marsh, S. H., & Smith, M. J. (2017). A comparison between London and Baghdad surface urban heat islands and possible engineering mitigation solutions. *Sustainable Cities and Society*, *29*, 159 – 168.
3. Alidadi, M., & Dadashpoor, H. (2018). Beyond monocentricity: examining the spatial distribution of employment in Tehran metropolitan region, iran. *International Journal of Urban Sciences*, *22*(1), 38–58.
4. Allegrini, J., Dorer, V., & Carmeliet, J. (2015). Influence of morphologies on the microclimate in urban neighbourhoods. *Journal of Wind Engineering and Industrial Aerodynamics*, *144*, 108 – 117.
5. Ardeshiri, A., Ardeshiri, M., Radfar, M., & Shormasty, O. H. (2016). The values and benefits of environmental elements on housing rents. *Habitat International*, *55*, 67 – 78.
6. Bagheri, B., & Tousi, S. N. (2018). An explanation of urban sprawl phenomenon in Shiraz metropolitan area (SMA). *Cities*, *73*, 71 – 90.
7. Barau, A. S., Maconachie, R., Ludin, A., & Abdulhamid, A. (2015). Urban morphology dynamics and environmental change in Kano, Nigeria. *Land Use Policy*, *42*, 307 – 317.
8. Barsi, J. A., Barker, J. L., & Schott, J. R. (2003). An atmospheric correction parameter calculator for a single thermal band earth-sensing instrument. In *Geoscience and Remote Sensing Symposium, 2003. IGARSS'03. Proceedings. 2003 IEEE International*, vol. 5, (pp. 3014–3016). IEEE.
9. Bokaie, M., Zarkesh, M. K., Arasteh, P. D., & Hosseini, A. (2016). Assessment of urban heat island based on the relationship between land surface temperature and land use/ land cover in Tehran. *Sustainable Cities and Society*, *23*, 94 – 104.
10. Boukhabla, M., Alkama, D., & Bouchair, A. (2013). The effect of urban morphology on urban heat island in the city of Biskra in Algeria. *International Journal of Ambient Energy*, *34*(2), 100–110.
11. Chander, G., & Markham, B. (2003). Revised landsat-5 tm radiometric calibration procedures and postcalibration dynamic ranges. *IEEE Transactions on geoscience and remote sensing*, *41*(11), 2674–2677.
12. Chen, X.-L., Zhao, H.-M., Li, P.-X., & Yin, Z.-Y. (2006). Remote sensing image-based analysis of the relationship between urban heat island and land use/cover changes. *Remote Sensing of Environment*, *104*(2), 133 – 146.
13. Clinton, N., & Gong, P. (2013). Modis detected surface urban heat islands and sinks: Global locations and controls. *Remote Sensing of Environment*, *134*, 294 – 304.
14. Connors, J. P., Galletti, C. S., & Chow, W. T. L. (2013). Landscape configuration and urban heat island effects: assessing the relationship between landscape characteristics and land surface temperature in Phoenix, Arizona. *Landscape Ecology*, *28*(2), 271–283.
15. Dihkan, M., Karsli, F., Guneroglu, A., & Guneroglu, N. (2015). Evaluation of surface urban heat island (SUHI) effect on coastal zone: The case of Istanbul megacity. *Ocean & Coastal Management*, *118*, 309 – 316.
16. Dugord, P. A., Lauf, S., Schuster, C., & Kleinschmit, B. (2014). Land use patterns, temperature distribution, and potential heat stress risk–the case study Berlin, Germany. Computers, Environment and Urban Systems, 48, 86-98.
17. Edussuriya, P., Chan, A., & Ye, A. (2011). Urban morphology and air quality in dense residential environments in Hong Kong. Part i: District-level analysis. *Atmospheric Environment*, *45*(27), 4789 – 4803.
18. Emmanuel, R., & Johansson, E. (2006). Influence of urban morphology and sea breeze on hot humid microclimate: the case of Colombo, Sri Lanka. *Climate research*, *30*(3), 189–200.
19. Ewing, R., Pendall, R., & Chen, D. (2002). Measuring sprawl and its impact: The character and consequences of metropolitan expansion. *Washington, DC: Smart Growth America*.
20. Frey, C. M., Rigo, G., & Parlow, E. (2005). Investigation of the daily urban cooling island (UCI) in two coastal cities in an arid environment: Dubai and Abu Dhabi (UAE). *City*, *81*, 2–06.
21. Grimmond, S. (2007). Urbanization and global environmental change: local effects of urban warming. *Geographical Journal*, *173*(1), 83–88.

ACCEPTED MANUSCRIPT

22. Guo, G., Zhou, X., Wu, Z., Xiao, R., & Chen, Y. (2016). Characterizing the impact of urban morphology heterogeneity on land surface temperature in Guangzhou, China. *Environmental Modelling & Software*, *84*, 427 – 439.
23. Hebbert, M. (2014). Climatology for city planning in historical perspective. Urban Climate, 10, 204-215.
24. Hu, Y., & Jia, G. (2010). Influence of land use change on urban heat island derived from multi-sensor data. *International Journal of Climatology*, *30*(9), 1382–1395.
25. Kahya, C., Bektas Balcik, F., Burak Oztaner, Y., & Guney, B. (2016). Determining land surface temperature relations with land use-land cover and air pollution. In *EGU General Assembly Conference Abstracts*, vol. 18, (p. 16489).
26. Keramitsoglou, I., Kiranoudis, C. T., Ceriola, G., Weng, Q., & Rajasekar, U. (2011). Identification and analysis of urban surface temperature patterns in greater Athens, Greece, using modis imagery. *Remote Sensing of Environment*, *115*(12), 3080 – 3090.
27. Kikon, N., Singh, P., Singh, S. K., & Vyas, A. (2016). Assessment of urban heat islands (UHI) of Noida city, India using multi-temporal satellite data. *Sustainable Cities and Society*, *22*, 19 – 28.
28. Lazzarini, M., Marpu, P. R., & Ghedira, H. (2013). Temperature-land cover interactions: The inversion of urban heat island phenomenon in desert city areas. *Remote Sensing of Environment*, *130*, 136 – 152.
29. Li, H., & Wu, J. (2004). Use and misuse of landscape indices. *Landscape Ecology*, *19*(4), 389–399.
30. Li, J., Song, C., Cao, L., Zhu, F., Meng, X., & Wu, J. (2011). Impacts of landscape structure on surface urban heat islands: A case study of shanghai, china. *Remote Sensing of Environment*, *115*(12), 3249 – 3263.
31. Li, X., Li, W., Middel, A., Harlan, S. L., Brazel, A. J., & Turner, B. L. (2016). Remote sensing of the surface urban heat island and land architecture in Phoenix, Arizona: Combined effects of land composition and configuration and cadastral–demographic–economic factors. *Remote sensing of environment*, *174*, 233-243.
32. Lilley, K. (2009). Urban morphology. In R. Kitchin, & N. Thrift (Eds.) *International Encyclopedia of Human Geography*, (pp. 66 – 69). Oxford: Elsevier.
33. Luo, D., Jin, H., Marchenko, S. S., & Romanovsky, V. E. (2018). Difference between near surface air, land surface and ground surface temperatures and their influences on the frozen ground on the Ginghai-Tibet plateau. *Geoderma*, *312*, 74 – 85.
34. McGarical, k., Chushan, S., Neel, M., & Ene, E. (2012). Spatial Pattern Analysis Program for Categorical and Continuous Maps. Computer software program produced by the authors. University of Massachusetts, Amherst. URL http://www.umass.edu/landeco/research/fragstats/fragstats.html
35. Mills, G. (2014). Urban climatology: History, status and prospects. Urban Climate, 10, 479-489.
36. Moonen, P., Defraeye, T., Dorer, V., Blocken, B., & Carmeliet, J. (2012). Urban physics: Effect of the micro-climate on comfort, health and energy demand. Frontiers of Architectural Research, 1(3), 197 – 228.
37. Morganti, M., Salvati, A., Coch, H., & Cecere, C. (2017). Urban morphology indicators for solar energy analysis. *Energy Procedia*, *134*, 807 – 814.
38. Ogashawara, I., & Bastos, V. d. S. B. (2012). A quantitative approach for analyzing the relationship between urban heat islands and land cover. *Remote Sensing*, *4*(11), 3596– 3618.
39. Oke, T. R. (1984). Towards a prescription for the greater use of climatic principles in settlement planning. *Energy and Buildings*, *7*(1), 1–10.
40. Peel, M. C., Finlayson, B. L., & McMahon, T. A. (2007). Updated world map of the Köppen-Geiger climate classification. Hydrology and earth system sciences discussions, 4(2), 439-473.
41. Petralli, M., Massetti, L., Brandani, G., & Orlandini, S. (2014). Urban planning indicators: useful tools to measure the effect of urbanization and vegetation on summer air temperatures. *International Journal of Climatology*, *34*(4), 1236–1244.
42. Privitera, R., Palermo, V., Martinico, F., Fichera, A., & Rosa, D. L. (2018). Towards lower carbon cities: urban morphology contribution in climate change adaptation strategies. *European Planning Studies*, *0*(0), 1–26.
43. Rahman, A., Aggarwal, S. P., Netzband, M., & Fazal, S. (2011). Monitoring urban sprawl using remote sensing and GIS techniques of a fast growing urban centre, India. *IEEE Journal of selected topics in applied earth observations and remote sensing*, *4*(1), 56–64.
44. Rasul, A., Balzter, H., & Smith, C. (2015). Spatial variation of the daytime surface urban cool island during the dry season in Erbil, Iraqi Kurdistan, from Landsat 8. *Urban Climate*, *14*(Part 2), 176–186.
45. Robinson, D. (2006). Urban morphology and indicators of radiation availability. *Solar Energy*, *80*(12), 1643 – 1648.
46. Salat, S. (2009). Energy loads, co2 emissions and building stocks: morphologies, typologies, energy systems and behaviour. *Building Research & Information*, *37*(5-6), 598–609.
47. Sarvestani, M. S., Ibrahim, A. L., & Kanaroglou, P. (2011). Three decades of urban growth in the city of Shiraz, Iran: A remote sensing and geographic information systems application. *Cities*, *28*(4), 320 – 329.
48. Sheng, L., Tang, X., You, H., Gu, Q., & Hu, H. (2017). Comparison of the urban heat island intensity quantified by using air temperature and Landsat land surface temperature in Hangzhou, china. *Ecological Indicators*, *72*, 738 – 746.
49. Sobrino, J. A., Jiménez-Muñoz, J. C., & Paolini, L. (2004). Land surface temperature retrieval from LANDSAT TM 5. Remote Sensing of environment, 90(4), 434-440.
50. Soltani, A., & Sharifi, E. (2012). A case study of sustainable urban planning principles in Curitiba (Brazil) and their applicability in Shiraz (Iran). *International Journal of Development and Sustainability*, *1*(2), 120–134.
51. Thani, S. K. S. O., Mohamad, N. H. N., & Abdullah, S. M. S. (2013). The influence of urban landscape morphology on the temperature distribution of hot-humid urban centre. Procedia-Social and Behavioral Sciences, 85, 356-367.
52. Tong, S., Wong, N. H., Jusuf, S. K., Tan, C. L., Wong, H. F., Ignatius, M., & Tan, E. (2018). Study on correlation between air temperature and urban morphology parameters in built environment in northern china. *Building and Environment*, *127*, 239 – 249.

ACCEPTED MANUSCRIPT

53. Tran, D. X., Pla, F., Latorre-Carmona, P., Myint, S. W., Caetano, M., & Kieu, H. V. (2017). Characterizing the relationship between land use land cover change and land surface temperature. *ISPRS Journal of Photogrammetry and Remote Sensing*, *124*, 119 – 132.
54. Tsirigoti, D., & Bikas, D. (2017). A cross scale analysis of the relationship between energy efficiency and urban morphology in the Greek city context. *Procedia Environmental Sciences*, *38*, 682 – 687.
55. Wei, R., Song, D., Wong, N. H., & Martin, M. (2016). Impact of Urban Morphology Parameters on Microclimate. Procedia Engineering, 169, 142-149.
56. Weng, Q., Liu, H., & Lu, D. (2007). Assessing the effects of land use and land cover patterns on thermal conditions using landscape metrics in city of Indianapolis, United States. *Urban Ecosystems*, *10*(2), 203–219.
57. Whitehand, J., & Gu, K. (2010). Conserving urban landscape heritage: a geographical approach. *Procedia - Social and Behavioral Sciences*, *2*(5), 6948 – 6953.
58. Wu, H., Ye, L.-P., Shi, W.-Z., & Clarke, K. C. (2014). Assessing the effects of land use spatial structure on urban heat islands using hj-1b remote sensing imagery in Wuhan, China. *International Journal of Applied Earth Observation and Geoinformation*, *32*, 67 – 78.
59. Xu, Y., Ren, C., Ma, P., Ho, J., Wang, W., Lau, K. K.-L., Lin, H., & Ng, E. (2017). Urban morphology detection and computation for urban climate research. *Landscape and Urban Planning*, *167*, 212 – 224.
60. Zha, Y., Gao, J., & Ni, S. (2003). Use of normalized difference built-up index in automatically mapping urban areas from tm imagery. *International Journal of Remote Sensing*, *24*(3), 583–594.
61. Zhang, J., & Wang, Y. (2008). Study of the relationships between the spatial extent of surface urban heat islands and urban characteristic factors based on Landsat ETM+ data. *Sensors*, *8*(11), 7453.
62. Zhou, D., Zhao, S., Liu, S., Zhang, L., & Zhu, C. (2014). Surface urban heat island in china's 32 major cities: Spatial patterns and drivers. *Remote Sensing of Environment*, *152*(Supplement C), 51–61.
63. Zhou, W., Huang, G., & Cadenasso, M. L. (2011). Does spatial configuration matter? Understanding the effects of land cover pattern on land surface temperature in urban landscapes. *Landscape and Urban Planning*, *102*(1), 54 – 63.
64. Zhou, Y., Zhuang, Z., Yang, F., Yu, Y., & Xie, X. (2017). Urban morphology on heat island and building energy consumption. *Procedia Engineering*, *205*, 2401 – 2406.

ACCEPTED MANUSCRIPT